Effects of Preplasma Scale Length and Laser Intensity on the Divergence of Laser-Generated Hot Electrons

V. M. Ovchinnikov,[1,2] D. W. Schumacher,[1] M. McMahon,[1] E. A. Chowdhury,[1] C. D. Chen,[3] A. Morace,[4,5] and R. R. Freeman[1]

[1]*The Ohio State University, Department of Physics, Columbus, Ohio 43210, USA*
[2]*Innovative Scientific Solutions Inc., 2766 Indian Ripple Road, Dayton, Ohio 45440, USA*
[3]*Lawrence Livermore National Laboratory, Livermore, California 94550, USA*
[4]*University of Milano, Dipartimento di Fisica, Milano 20133, Italy*
[5]*Center for Energy Research, University of California San Diego, La Jolla, California 92093, USA*

(Received 29 August 2012; published 8 February 2013)

We report on a numerical study of the effects of preplasma scale length and laser intensity on the hot-electron (≥ 1 MeV) divergence angle using full-scale 2D3V (two dimensional in space, three dimensional in velocity) simulations including a self-consistent laser-plasma interaction and photoionization using the particle-in-cell code LSP. Our simulations show that the fast-electron divergence angle increases approximately linearly with the preplasma scale length for a fixed laser intensity. On the other hand, for a fixed preplasma scale length, the laser intensity has little effect on the divergence angle in the range between 10^{18} and 10^{21} W/cm^2. These findings have important implications for the interpretation of experimental results.

DOI: 10.1103/PhysRevLett.110.065007 PACS numbers: 52.38.Kd, 52.57.Kk

The interaction of powerful lasers with solid targets is an area of intense study. Laser-generated hot electrons, electrons with kinetic energy at or above 1 MeV, are at the heart of many applications, for example, ion acceleration [1], new x-ray and positron sources [2], fast ignition [3], and the generation of warm dense matter [4]. The nature of the generation process and the resulting energy distribution of the hot electrons remains a subject of considerable interest [5,6]. Similarly, the angular distribution of the hot-electron flux is still not understood, or even well characterized, although it plays a key role in determining the efficiency with which hot electrons can be used to convey energy into a target. This is due to the multiplicity of techniques [7,8], that have been used to try to measure the angular distribution, the wide range of intensities and target types employed by various researchers, and the use of differing laser systems whose pulse characteristics are not always fully characterized. Indeed, over roughly the last two decades, experimental results of hot-electron full divergence angles ranging from 18° to 180° have been reported [9,10]. Understanding the electron divergence is essential for controlling it, a topic of considerable interest. Several techniques have been proposed to optimize the electron divergence including structured guiding [11], double pulse [12], magnetic switchyard [13], etc.

Recently, the comparison of K_α imaging to particle-in-cell (PIC) simulations has become prominent. The divergence values experimentally derived are inevitably significantly smaller than the predictions from PIC [7,14]. We have recently shown that PIC simulations, if they model full-scale targets over a sufficient time for the K_α image to completely form (10–20 ps), clearly demonstrate that the laser-plasma interaction (LPI) gives rise to large *electron* angular spreads with angles up to 70° *as well as* time integrated K_α images indicative of a smaller divergence [15]. We have shown that these two results are consistent, due primarily to the role electron refluxing plays in determining the time integrated K_α images. In so doing, we were able to benchmark our approach using a range of different targets, including buried cones and slabs with get-lost-layers and fully refluxing slabs. In this Letter, we now examine the angular distribution over an important range of parameters relevant to current studies and applications.

Except in cases where the laser pulse has virtually no prepulse [16], excitation during the leading edge gives rise to preplasma, forming an underdense interface between vacuum and the solid target. This preplasma is suspected to play a crucial role in the size of the observed hot-electron divergence but is almost never directly measured [17]. While preplasma is known to have a large effect on laser absorption [18] and the hot-electron spectrum [19], so far there has not been a study showing a clear, quantitative connection between the preplasma and electron divergence.

A recent report has asserted that the hot-electron divergence increases with laser intensity [20]. This conclusion was based on a careful compilation of experimental data obtained by different research groups who used a wide range of intensities. These compiled experimental results were from experiments conducted on different laser systems, inevitably with differing pulse characteristics, and employing different target geometries. Some experiments used ''sandwich'' targets with thin fluor layers in the middle while others used targets made from a single

material which meant that different techniques had to be used to extract the electron beam size [8]. Given the difficulty of comparing different experiments to each other, the low statistics of some results due to the low repetition rate of the lasers used and, as we have shown [15,21], the key role played by target geometry in shaping the response of experimental diagnostics, the dependence of the hot-electron divergence on laser intensity remains unresolved.

In this Letter, we report the results of full-scale 2D simulations including a fully self-consistent laser-plasma interaction and Ammosov-Delone-Krainov photoionization using the PIC code LSP [22]. Our simulations show that the divergence increases approximately linearly with the preplasma scale length for a fixed laser intensity. Moreover, we find that the hot-electron divergence angle has little or no dependence on laser intensity in the range between 10^{18} W/cm^2 and 10^{21} W/cm^2 contrary to simple expectations based on a peak-intensity-derived ponderomotive ejection angle [23]. Together, these results are important for understanding experiments where changing the laser intensity also changes the size (and possibly the timing) of prepulse allowing what is, in fact, preplasma intensity dependence to be mistaken for laser intensity dependence.

Our basic approach to these simulations has been described previously [15] and Fig. 1 shows the geometry used. Briefly, these all kinetic simulations are performed in 2D Cartesian using a direct-implicit advance and an energy-conserving particle push that eliminates numerical

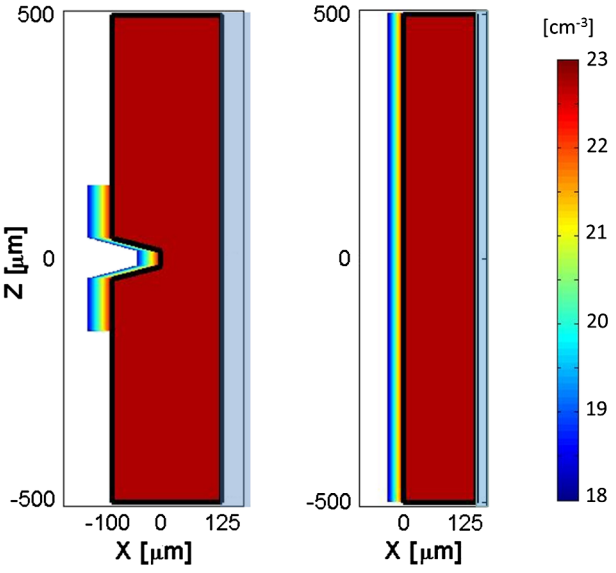

FIG. 1 (color online). Simulation geometry for the buried cone target (left) and the flat target (right). The black line indicates the solid density contour, the grey line the simulation grid. The color scale on the right shows electron number density in cm^{-3} (log scale). The laser is incident from the left and focused at the origin. The light blue color represents a region that absorbs electrons (see Ref. [15]). Each simulation ran for 10 ps.

heating due to large cell size. Transport effects are important for these simulations since return current and resistive fields affect the angular distributions, even measured close to the LPI region, so the transport modeling procedure developed in previous work was used. Here we treat buried cone targets since their use in our simulations is now well benchmarked by extensive comparison to experiment [15]. We also treat slabs and present new experimental data. There are two key differences from past work, however. First, although K_α images are well resolved using $\lambda/8$ sized cells (laser wavelength $\lambda = 1$ μm), resolving the electron dynamics in the region of the LPI requires $\lambda/16$. (We have run with $\lambda/32$ and observe little difference.) Second, we have added an Ammosov-Delone-Krainov photoionization model to LSP and laser ionization was modeled sequentially from singly ionized through all ionization stages on each time step [24,25]. To systematically model the effect of preplasma, preplasma filled the cone following an exponential density profile, $\rho = \rho_0 e^{-d/L}$, where ρ_0 is solid density, L is the preplasma scale length, and d is the distance from the solid density interface. The preplasma extended at least 50 μm from the solid density interface and spanned nearly 5 orders of magnitude in density.

The laser pulse modeled for this work was similar to that of the Titan Laser (Lawrence Livermore National Laboratory) and had a wavelength of $\lambda = 1$ μm with a sine-squared temporal intensity profile. The laser pulse delivered an equivalent of 150 J of energy to a 14 μm (intensity FWHM) focal spot in 700 fs (intensity FWHM). The transverse spatial profile was Gaussian with a variable peak intensity between 10^{18} and 10^{21} W/cm^2 in vacuum. The laser propagation direction was in the $+x$ direction, incident from the left boundary of the grid, and the laser was polarized in the z direction.

Our previous work has demonstrated an excellent match between experimentally recorded $K\alpha$ images using buried cone targets and our simulations [15]. Figure 2 shows a comparison between new, recent experimental results from Titan, but using flat targets at 10^{20} W/cm^2 and simulations. The black line indicates the experimental $K\alpha$ data, red the simulation. Fluor depths from left to right are 15, 100, and 200 μm, respectively. Again, we see good agreement.

After benchmarking our code against experimental data we can now use our simulations to focus on the *electron* angular divergence—something we cannot easily measure in an experiment. There are multiple approaches by which the electron distribution can be characterized [14]. For this work, we determined the electron divergence for a given value of the preplasma scale length by measuring the hot-electron spot size (FWHM) at three target depths ($x = 0$ μm, 50 μm and 100 μm). The spot size growth was fit to a line and the full divergence angle was then determined from the slope. This approach was chosen because it provides a useful measure for how well the hot electrons can carry energy into the forward direction, a key

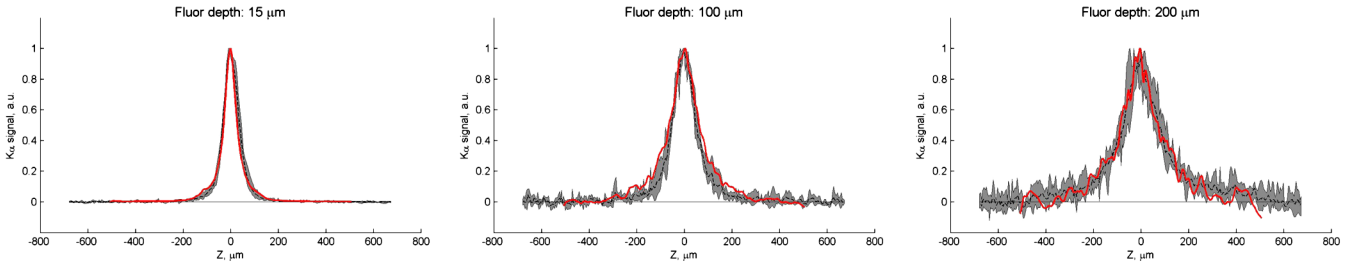

FIG. 2 (color online). Comparison between experimental $K\alpha$ (black) and the data obtained from the simulations (red) for flat targets. Fluor depths from left to right are 15, 100, and 200 μm. The range in the experimental data is shown as a gray band.

parameter for many applications. The results are shown in Fig. 3, where we see a clear, approximately linear dependence of divergence angle on scale length. The error for each fit is indicated. We find that the divergence angle increases about $7.0° \pm 0.6°$ for an increase in scale length of 1 μm.

The laser deposits most of its energy at the plasma relativistic critical surface and the larger the preplasma scale length, the further the critical surface is from the target. For longer scale lengths, the electrons excited by the laser have to travel a larger distance to reach the same depth inside the target and, since the electron beam is diverging, this has the effect of increasing the electron spot size at all depths but does not in itself change the divergence angle. However, in addition to shifting the critical surface away from the solid density surface, a larger preplasma scale length permits the laser to interact with the preplasma at densities close to critical over a larger range of distances due to curvature of the critical surface caused by relativistic transparency.

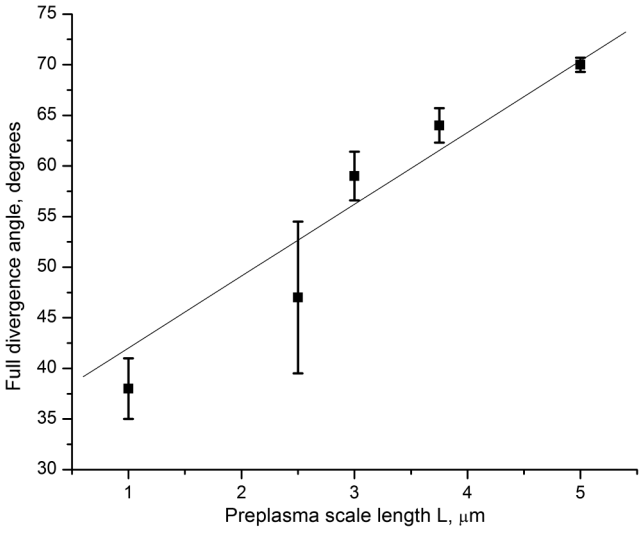

FIG. 3. Electron beam divergence vs preplasma scale length for buried cone target simulations. Each point and error bar is derived from the growth of the electron spot size at three different depths. The black curve is a linear fit. Divergence angle increases $7.0° \pm 0.6°$ for each 1 μm increase of scale length L.

Debayle *et al.* [14] provide an appealing physical argument relating the hot-electron divergence to the preplasma conditions. Part of the origin of the inherent electron divergence is the transverse component of the laser ponderomotive force. For the case of a short scale length, electrons are generated roughly at the same distance from solid density across the beam profile. However, in the case of a longer scale length, the effective interaction range is much larger because of the curvature of the relativistic critical surface due to the laser intensity variation. This causes a much larger variation in the electron transverse velocity component. In addition, the size and the strength of the quasistatic magnetic fields formed by the Weibel instability in the case of a longer scale length are larger compared to the small scale length case. These fields help scatter electrons much more effectively leading to a higher divergence [14]. Debayle *et al.* [14] estimated that the *local* mean propagation angle depends on the length of the interaction region L_i as

$$\theta_r \approx \frac{rL_i}{2r_0^2}\Delta\theta_0^2,$$

where r is the transverse direction, r_0 is the initial size of the electron beam, $\Delta\theta_0$ is the electron distribution dispersion angle, and the local propagation angle at a given point is defined as $\theta_r = \tan^{-1}(p_x/p_z)$, where p_x and p_z are the transverse and longitudinal components of the momentum. Unless the laser Rayleigh range is small compared to the scale length, r_0 is approximately constant. Debayle *et al.* assume a constant dispersion angle $\Delta\theta_0$. In our simulations we find $\Delta\theta_0$ to be constant over the central portion of the laser where most hot electrons are generated with a value approximately equal to 35°. For an exponential preplasma profile, the length of the interaction region L_i is related to the preplasma scale length L as $L_i = L\ln\gamma$, where γ is the Lorentz factor. Finally, the electron full divergence angle, the main subject of this study, will be proportional to the local mean propagation angle evaluated at $r = r_0$. These considerations suggest that the full divergence angle should be linearly proportional to the preplasma scale length:

$$\theta_{\text{full div}} \sim 2\theta_{r,\text{bal}}(r = r_0) = \frac{L\ln(\gamma)}{r_0}\Delta\theta_0^2 \sim L,$$

consistent with the trend seen in our simulations.

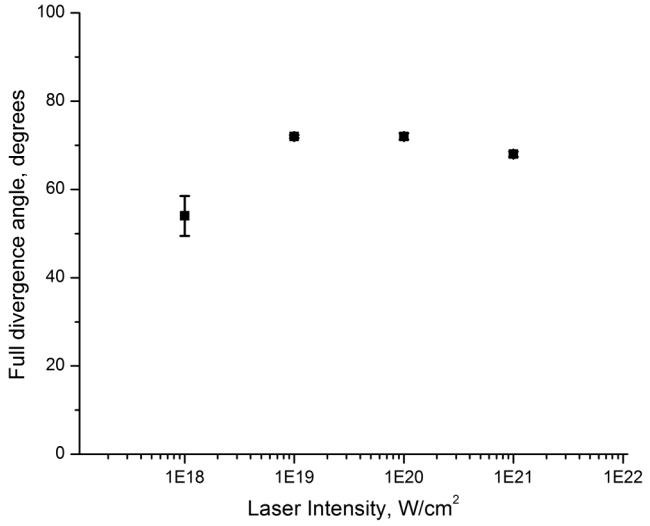

FIG. 4. Electron beam divergence vs laser intensity. The divergence angle was determined by the same method as in Fig. 3. Error bars on the graph are from the fitting errors.

We now turn to the dependence of the divergence angle on laser intensity. Here, we performed a series of simulations similar to the ones described above, but for a fixed preplasma scale length of $L = 3$ μm with the intensity varying over three orders of magnitude from 10^{18} W/cm^2 to 10^{21} W/cm^2. To be consistent with the experiments used in Green *et al.* [20], the target was a flat foil 1 mm wide and 150 μm thick. All other parameters were identical to the previous simulations. The results are shown in Fig. 4. We find a nearly constant divergence angle of $\sim 70°$ whereas Green *et al.* finds that the divergence angle increases monotonically with the laser intensity. To our knowledge, none of the experiments in Ref. [20] report monitoring laser prepulse so it is possible the effect that Green *et al.* reports was not due to the laser intensity itself but due to an increasing preplasma scale length caused by increasing *prepulse* energy.

In conclusion, we have performed a numerical study of the effect of preplasma scale length and laser intensity on the hot-electron divergence angle using full scale 2D3V simulations using the PIC code LSP. Our results indicate that the fast-electron divergence angle increases nearly linearly with the preplasma scale length for a fixed laser intensity. This can be explained by a larger interaction volume being available for longer scale lengths. We also found that for a fixed preplasma scale length, the laser intensity had little effect on the divergence angle in the range between 10^{18} W/cm^2 and 10^{21} W/cm^2. Since the prepulse intensity can increase with increasing pulse intensity, depending on the mechanism by which the intensity is varied, it is possible that a higher laser intensity would produce a longer scale length preplasma that would indeed yield a larger electron divergence angle. In general, different laser systems will have different levels of prepulse for the same intensity. Thus, it may not be valid to combine results from different systems to determine electron divergence.

We thank Dr. Michael Storm and Douglas Wertepny for helpful discussion. This work was performed with support from the DOE under Contracts No. DE-FG02-05ER54834 and No. DE-AC52-07NA27344, and allocations of computing time from the Ohio Supercomputer Center and the Lawrence Livermore National Laboratory (LLNL) Institutional Computing Grand Challenge program.

[1] R. A. Snavely *et al.*, Phys. Rev. Lett. **85**, 2945 (2000).
[2] H. Chen, S. Wilks, J. Bonlie, E. Liang, J. Myatt, D. Price, D. Meyerhofer, and P. Beiersdorfer, Phys. Rev. Lett. **102**, 105001 (2009).
[3] M. Tabak, J. Hammer, M. E. Glinsky, W. L. Kruer, S. C. Wilks, J. Woodworth, E. M. Campbell, M. D. Perry, and R. J. Mason, Phys. Plasmas **1**, 1626 (1994).
[4] M. Koenig *et al.*, Plasma Phys. Controlled Fusion **47**,B441 (2005).
[5] T. Ma *et al.*, Phys. Rev. Lett. **108**, 115004 (2012).
[6] T. Kluge, T. Cowan, A. Debus, U. Schramm, K. Zeil, and M. Bussmann, Phys. Rev. Lett. **107**, 205003 (2011).
[7] R. B. Stephens *et al.*, Phys. Rev. E **69**, 066414 (2004).
[8] K. L. Lancaster *et al.*, Phys. Rev. Lett. **98**, 125002 (2007).
[9] H. Popescu *et al.*, Phys. Plasmas **12**, 063106 (2005).
[10] K. B. Wharton, S. Hatchett, S. Wilks, M. Key, J. Moody, V. Yanovsky, A. Offenberger, B. Hammel, M. Perry, and C. Joshi, Phys. Rev. Lett. **81**, 822 (1998).
[11] A. P. L. Robinson and M. Sherlock, Phys. Plasmas **14**, 083105 (2007).
[12] A. P. L. Robinson, M. Sherlock, and P. A. Norreys, Phys. Rev. Lett. **100**, 025002 (2008).
[13] A. P. L. Robinson, M. H. Key, and M. Tabak, Phys. Rev. Lett. **108**, 125004 (2012).
[14] A. Debayle, J. J. Honrubia, E. d'Humières, and V. T. Tikhonchuk, Phys. Rev. E **82**, 036405 (2010).
[15] V. M. Ovchinnikov, D. W. Schumacher, G. E. Kemp, A. G. Krygier, L. D. Van Woerkom, K. U. Akli, R. R. Freeman, R. B. Stephens, and A. Link, Phys. Plasmas **18**, 112702 (2011).
[16] R. C. Shah, R. P. Johnson, T. Shimada, K. A. Flippo, J. C. Fernandez, and B. M. Hegelich, Opt. Lett. **34**, 2273 (2009).
[17] S. Le Pape *et al.*, Opt. Lett. **34**, 2997 (2009).
[18] Y. Ping *et al.*, Phys. Rev. Lett. **100**, 085004 (2008).
[19] A. G. MacPhee *et al.*, Phys. Rev. Lett. **104**, 055002 (2010).
[20] J. S. Green *et al.*, Phys. Rev. Lett. **100**, 015003 (2008).
[21] V. M. Ovchinnikov, G. E. Kemp, D. W. Schumacher, R. R. Freeman, and L. D. Van Woerkom, Phys. Plasmas **18**, 072704 (2011).
[22] D. R. Welch, D. V. Rose, R. E. Clark, T. C. Genoni, and T. P. Hughes, Comput. Phys. Commun. **164**, 183 (2004).
[23] P. Gibbon, *Short Pulse Laser Interaction with Matter: An Introduction*, (Imperial College Press, London, 2005).
[24] A. M. Perelomov, V. S. Popov, and M. V. Terent'ev, Zh. Eksp. Teor. Fiz. **50**, 1393 (1966) [Sov. Phys. JETP **23**, 924 (1966)].
[25] M. V. Ammosov, N. B. Delone, and V. P. Krainov, Zh. Eksp. Teor. Fiz. **91**, 2008 (1986) [Sov. Phys. JETP **64**, 1191 (1986)].